ChemPubSoc Europe
DOI: 10.1002/chem.201601918
CHEMISTRY A European Journal
Full Paper

Redox Chemistry

Effect of Molecular Interactions on Electron-Transfer and Antioxidant Activity of Bis(alkanol)selenides: A Radiation Chemical Study

Pavitra V. Kumar,[a, b] Beena G. Singh,*[a] Prasad P. Phadnis,[c] Vimal K. Jain,[b, c] and K. Indira Priyadarsini*[a, b]

Abstract: Understanding electron-transfer processes is crucial for developing organoselenium compounds as antioxidants and anti-inflammatory agents. To find new redox-active selenium antioxidants, we have investigated one-electron-transfer reactions between hydroxyl (ˑOH) radical and three bis(alkanol)selenides (SeROH) of varying alkyl chain length, using nanosecond pulse radiolysis. ˑOH radical reacts with SeROH to form radical adduct, which is converted primarily into a dimer radical cation ($(>\mathrm{Se}\therefore\mathrm{Se}<)^+$) and α-{bis-(hydroxyl alkyl)}-selenomethine radical along with a minor quantity of an intramolecularly stabilized radical cation. Some of these radicals have been subsequently converted to their corresponding selenoxide, and formaldehyde. Estimated yield of these products showed alkyl chain length dependency and correlated well with their antioxidant ability. Quantum chemical calculations suggested that compounds that formed more stable $(>\mathrm{Se}\therefore\mathrm{Se}<)^+$, produced higher selenoxide and lower formaldehyde. Comparing these results with those for sulfur analogues confirmed for the first time the distinctive role of selenium in making such compounds better antioxidants.

Introduction

Excessive production of reactive oxygen species (ROS) leads to loss of redox balance in cells, which is considered to be responsible for the onset of several chronic diseases like inflammation, cancer, ageing etc., and antioxidants are recommended to maintain cellular redox homeostasis.[1] Sulfur and selenium compounds, both from natural and synthetic sources, are finding use as antioxidants and anti-inflammatory agents and are being explored as a new class of drugs for preventing and treatment of diseases.[2,3] Selenium is unique in that it is an important micronutrient and is a constituent of crucial redox-regulating enzymes like glutathione peroxidase (GPx) and thioredoxin reductase (TrxR).[4,5] Preferential application of selenium as redox modulator emerges from its ability to exhibit a range of oxidation states and a variety of redox reactions. Although sulfur and selenium share the same group, their chemistry is distinctly different.[6] For example, due to a higher covalent radius, selenium can interact with its neighboring heteroatom through nonbonding interactions, which influences the electron density on the selenium atom, thereby modulating its ability to participate in the redox reactions.[7,8] We have been investigating the nature and reactivity of selenium-centered radicals generated by hydroxyl (ˑOH) radical reactions on a variety of organoselenium compounds ranging from simple selenourea to bifunctional seleno-amino acids like selenomethione and selenocystine.[9–12] For all the chosen compounds, the ˑOH radical was found to react with the selenium atom; the nature, stability and reactivity of the resulting selenium radicals are modulated by nonbonding interactions between selenium and the neighboring heteroatom.[9–11]

Another important property of selenium compounds is their ability to exhibit GPx-like activity where it catalyzes the reduction of hydrogen peroxide, a molecular oxidant and ROS.[13,14] For a designed organoselenium compound to be an antioxidant, it should not only show GPx-like activity but also exhibit free-radical reactions and the reaction products of such reactions are recyclable. Previous studies on the antioxidant activities of both aliphatic as well as aromatic selenium compounds showed that the free-radical scavenging ability and the GPx activity do not correlate as the former proceeds through one-electron transfer while the latter takes place by two-electron or oxygen transfer.[9,15] In the present investigation, we propose for the first time that one-electron-transfer processes in simple aliphatic bis(alkanol)selenide (SeROH; Scheme 1) can generate products that are redox cycled and participate in GPx antioxi-

---

[a] P. V. Kumar, Dr. B. G. Singh, Dr. K. I. Priyadarsini
Radiation and Photochemistry Division
Bhabha Atomic Research Centre, Trombay, Mumbai, 400085 (India)
E-mail: beenam@barc.gov.in
kindira@barc.gov.in

[b] P. V. Kumar, Dr. V. K. Jain, Dr. K. I. Priyadarsini
Homi Bhabha National Institute, Anushaktinagar, Mumbai, 400094 (India)

[c] Dr. P. P. Phadnis, Dr. V. K. Jain
Chemistry Division, Bhabha Atomic Research Centre
Trombay, Mumbai, 400085 (India)

Supporting information for this article is available on the WWW under http://dx.doi.org/10.1002/chem.201601918.

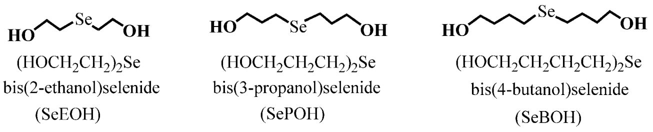

Scheme 1. Chemical structure of the SeROH compounds.

dant activity. For this, detailed pulse radiolysis studies on the reaction of $^{\bullet}$OH radical with SeROH were carried out, the products were estimated and the results were complimented by quantum chemical calculations.

Results and Discussion

1. Pulse radiolysis studies

The reaction of SeROH with $^{\bullet}$OH radical results in the formation of different types of selenium-centered radicals and these transients were characterized by monitoring their spectral and kinetic properties under different experimental conditions like pH, proton and SeROH concentration. The results from individual alcohol are presented below.

Bis(2-ethanol)selenide (SeEOH)

Reaction of SeEOH with $^{\bullet}$OH radicals produced a transient that showed absorption spectrum in the wavelength range of 200 to 600 nm and was found to be different at various concentrations of SeEOH (Figure 1). At 100 μM, the transient spectrum showed a small peak at 320 nm and another intense absorption band with a maximum at 490 nm. Increasing the concentration to 1 or 2.5 mM, generated a similar spectral pattern, however the absorbance at 490 nm increased significantly, while that at 320 nm was little influenced. The concentration-dependent absorbance at 490 nm is attributed to the dimer radical of the type $(>\text{Se}\therefore\text{Se}<)^{+}$ formed by the reaction of selenium-centered radical cation $(>\text{Se}^{\bullet+})$ with parent SeEOH, as observed (path IIc and IIIa in Scheme 2) with most sulfur and selenium radical cations, through two-centered-three-electron (2c–3e) hemibond formation involving the p-orbital of the $(>\text{Se}^{\bullet+})$ with the p-orbital containing the lone pair of electrons of the other selenium atom of SeEOH.[9–11] The absorption band at 320 nm may be either due to the formation of $(>\text{Se}\therefore\text{OH})$ (path I in Scheme 2) or selenium-centered radical cation $(>\text{Se}^{\bullet+})$ (path II a/b in Scheme 2).

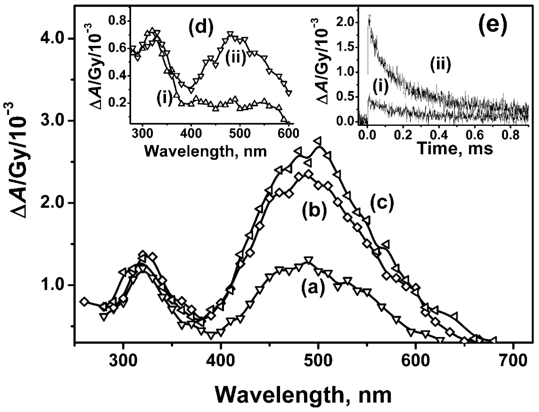

Figure 1. Transient spectra obtained at 10 μs after pulse radiolysis of N_2O-saturated aqueous solutions of: a) 100 μM, b) 1 mM, and c) 2.5 mM SeEOH at pH 7. Inset d: the decay traces at: i) 320 nm, and ii) 490 nm obtained during the reaction of the $^{\bullet}$OH radical with 1 mM SeEOH. Inset e: time-resolved transient spectra of 50 μM SeEOH obtained at: i) 1 μs, and ii) 20 μs after the pulse. Absorbed dose, (9.9 ± 0.2) Gy.

To distinguish these different species, their decay at 320 and 490 nm was monitored in the presence of phosphate ion (proton donor). If the species is $(>\text{Se}\therefore\text{OH})$, it decays to $(>\text{Se}^{\bullet+})$ by the loss of water which is expected to be accelerated at higher proton concentrations.[16,17] To understand this, the concentration of SeEOH was fixed at 100 μM SeEOH and the dihydrogenphosphate ($H_2PO_4^-$) ion concentration was varied from 5 to 50 mM. The absorbance at 490 nm increased

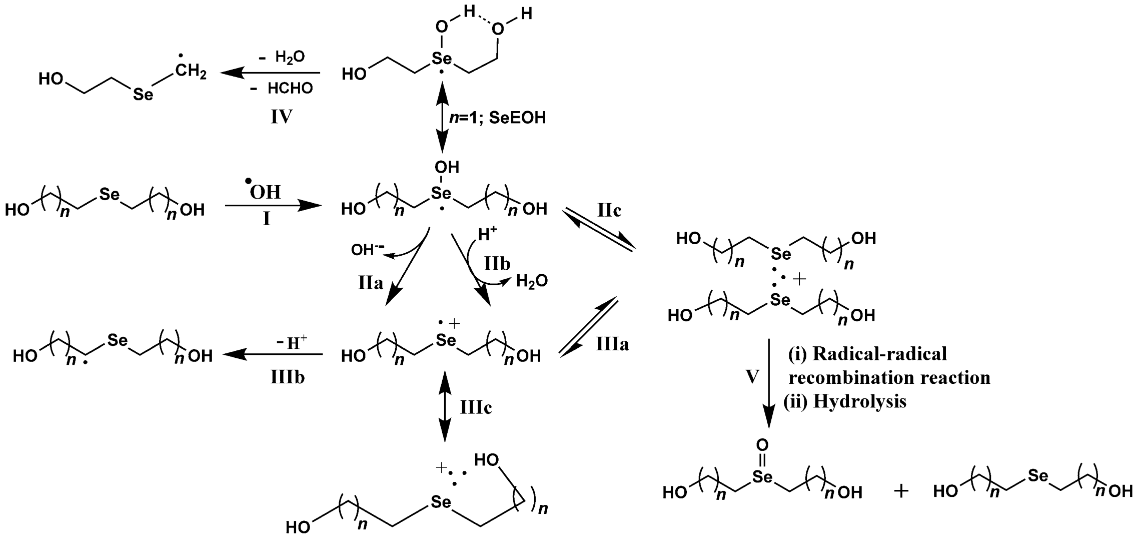

Scheme 2. Proposed mechanism for the possible reactions of the $^{\bullet}$OH radical with SeROH.

with increasing $H_2PO_4^-$ concentration, while that at 320 nm did not change. Thus the absorbance at 320 nm is ruled out to be from ($>$Se$\therefore$OH) radical. To further confirm this, the transient spectrum was recorded for the reaction of SeEOH with $^{\bullet}$OH radical at pH 1. For this study, the concentration of SeEOH was kept at 50 μм, so that high proton and low SeEOH concentration would favor formation of ($>$Se$^{\bullet+}$). The transient spectrum at pH 1, showed an absorption maximum only at 490 nm, while the absorption band at 320 nm was not observed (Figure S1 in the Supporting Information), clearly confirming that the transient absorbing at 320 nm is neither due to ($>$Se$\therefore$OH) nor ($>$Se$^{\bullet+}$). On close observation of the decay and formation kinetics of the 320 nm absorbing species as a function of SeEOH and proton concentration, it can be inferred that this absorption band is formed very fast ($<$1 μs) as compared to the ($>$Se$\therefore$Se$<$)$^+$ radical, and is not the precursor or successor of ($>$Se$\therefore$Se$<$)$^+$ radical (inset d, Figure 1). The absorbance at 320 nm decayed by following first-order kinetics with a rate constant of $(3.8\pm0.2)\times10^3\ s^{-1}$, while that at 490 nm decayed by second-order kinetics with $2k/\varepsilon$value of $(9.4\pm0.3)\times10^5\ s^{-1}$ (inset e, Figure 1) indicating radical–radical dismutation reaction. From these results, the 320 nm absorbing species can be envisaged to be a carbon-centered radical of the type α-(hydroxylethyl)seleno methyl radical ($HOCH_2CH_2SeCH_2^{\bullet}$). Such radicals can be formed by rearrangement of ($>$Se$\therefore$OH) at α-position to the selenium center as reported for similar sulfur compound (path IV, Scheme 2).[18] In summary the observable transient spectra of SeEOH at 320 and 490 nm were attributed to ($HOCH_2CH_2SeCH_2^{\bullet}$) and ($>Se\therefore$Se$<$)$^+$ radicals, respectively.

Bis(3-propanol)selenide (SePOH)

Similar to SeEOH, the reaction of $^{\bullet}$OH radical with SePOH produced a concentration-dependent transient spectrum (plots a–c, Figure 2). At 50 μм, the transient spectrum is broad in the range from 200 to 600 nm with the absorption maximum at around 370 nm. On increasing the concentration of SePOH to 100 μм, clear time-resolved changes in the absorption spectra were observed (inset, Figure 2). Here, the broad absorption maximum at 350–370 nm seen at 1 μs, decayed with the formation of new absorption maximum at 500 nm (inset, Figure 2) at 40 μs after the pulse.

On increasing the concentration of SePOH to 250 μм (Figure 2b), the 370 nm band was absent, while the broad band in the wavelength range above 400 nm increased, but showed a split in the band with two maxima at 460 and 500 nm and at 1 mм only increase in the absorbance at both the wavelengths was observed. To assign these bands, experiments were performed at different concentration of $H_2PO_4^-$ and SePOH. At 100 μм SePOH, the spectrum in nanopure water (plot a, Figure 3) showed only the transient absorbance at 370 nm, while in the presence of $H_2PO_4^-$ the 370 nm peak was absent with formation of 500 nm absorbing species (plot b, Figure 3). Inset c of Figure 3 shows loss of absorbance at 370 nm correlating with the increase in the 500 nm species and with increasing $H_2PO_4^-$ concentration. This indicates that the transient absorbance at 370 nm is due to the ($>$Se$\therefore$OH) radical, which decays faster in the presence of a proton donor like $H_2PO_4^-$ to form ($>$Se$^{\bullet+}$), that is converted to ($>$Se$\therefore$Se$<$)$^+$ radical, by reaction with SePOH. As observed in sulfur-centered radical reactions, ($>$Se$\therefore$OH) may also directly react with the parent molecule to give ($>$Se$\therefore$Se$<$)$^+$ radical and OH^-. Therefore, the dependence of the absorbance at 370 and 500 nm was also studied as a function of SePOH concentration. For these studies, the experiment was conducted in nanopure water, without any added phosphate ion while the concentration of SePOH was changed. With increasing SePOH concentration the absorbance at 370 nm decreased with concomitant increase in the absorbance at 500 nm (inset d, Figure 3). By comparing the data with other selenium compounds, the transient absorbance at 500 nm was assigned to a ($>$Se$\therefore$Se$<$)$^+$ radical (paths IIc and IIIa, Scheme 2).

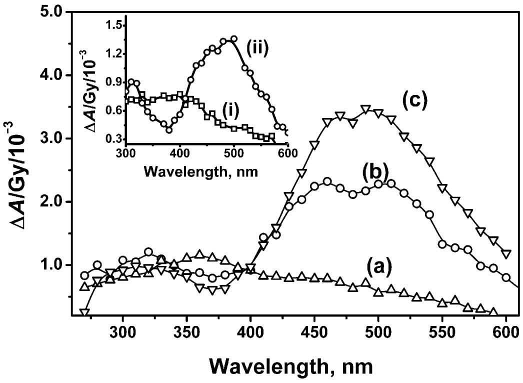

Figure 2. Transient spectra obtained at 5 μs after pulse radiolysis of N_2O-saturated aqueous solutions of: a) 50 μм, b) 250 μм, and c) 1 mм SePOH at pH 7. Inset: the time-resolved transient spectra of 100 μм SePOH obtained at: i) 1 μs, and ii) 40 μs after the pulse. Absorbed dose, (9.9 ± 0.3) Gy.

An unusual behavior was observed in SePOH, where along with the absorbance at 500 nm, an additional peak at 460 nm was noticed at 250 μм. Like the 500 nm absorbing species, this 460 nm transient too increased with increasing parent concentration and decayed by second-order decay kinetics, but they

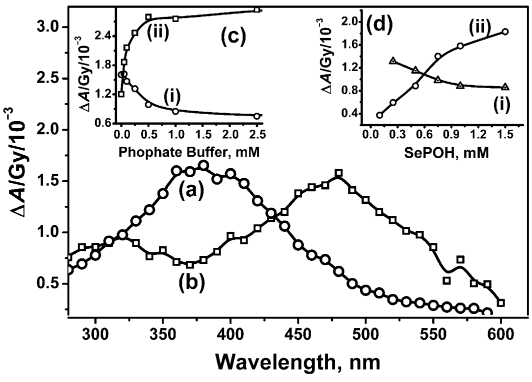

Figure 3. Transient spectra obtained at 20 μs after pulse radiolysis of N_2O-saturated aqueous solutions of 100 μм SePOH at pH 7, in: a) the absence, and b) presence of 5 mм phosphate buffer. Insets c and d: change in absorbance at: i) 370 nm, and ii) 500 nm as a function of phosphate buffer (SePOH = 100 μм) and SePOH concentration (in the absence of buffer), respectively. Absorbed dose, (10.4 ± 0.3) Gy.

differ in their half-life (decay pattern shown in Figure S2 in the Supporting Information) indicating that even though both the transients are formed by association of the selenium radical with parent molecule, they appear to have different structures. This was further confirmed by performing the experiments with azide ($N_3^{\bullet}$) radical, a specific one-electron oxidant.[19] The transient spectrum generated on treatment of 6 mм SePOH with $N_3^{\bullet}$ radical at pH 7, showed only one peak with a maximum at 460 nm and the decay of the absorption-time plot at both 460 and 500 nm was similar (Figure S3 in the Supporting Information), unlike that observed with the ${}^{\bullet}$OH radical. From this it can be inferred that the transient absorbing at 460 nm is due to the $(>\mathrm{Se}\therefore\mathrm{Se}<)^+$ radical, while that absorbing at 500 nm may be due to association of the $(>\mathrm{Se}\therefore\mathrm{OH})$ adduct with the parent SePOH. From these studies it can be inferred that $(>\mathrm{Se}\therefore\mathrm{OH})$ absorbing at 370 nm undergoes multiple reaction pathways such as spontaneous dissociation (path IIa, Scheme 2), acid catalyzed elimination of hydroxide ion (path IIb, Scheme 2) and reaction with another SePOH molecule (path IIc, Scheme 2). No detailed decay analysis was attempted.

Bis(4-butanol)selenide (SeBOH)

As seen in other derivatives, reaction between 50 μм SeBOH and the ${}^{\bullet}$OH radical gave a transient spectrum in the wavelength range from 200 to 600 nm, with two absorption maxima, a weekly absorbing species at 320 nm and a strong band at 500 nm. The spectra recorded at different concentrations of SeBOH (50, 100 and 500 μм, plots a, b and c, respectively, Figure 4) indicated that the absorbance at 500 nm, increased with increasing SeBOH concentration, due to the $(>\mathrm{Se}\therefore\mathrm{Se}<)^+$ radical (paths IIc and IIIa, Scheme 2), and the absorbance at 320 nm remained unchanged. At pH 1, the ${}^{\bullet}$OH radical reaction with SeBOH (500 μм) produced only the $(>\mathrm{Se}\therefore\mathrm{Se}<)^+$ radical (Figure S4). Further, SeBOH reacted with $N_3^{\bullet}$ to generate a transient absorption spectrum with an absorption maximum at 500 nm, confirming that the transient is a $(>\mathrm{Se}\therefore\mathrm{Se}<)^+$ radical (Figure S5 in the Supporting Information). On the contrary, the 320 nm absorbing species was formed in less than 3 μs and its decay is slower than that of the $(>\mathrm{Se}\therefore\mathrm{Se}<)^+$ radical absorbing at 500 nm. This result indicates that the species absorbing at 320 nm is independent of the $(>\mathrm{Se}\therefore\mathrm{Se}<)^+$ radical, however, due to a low extinction coefficient, it was difficult to carry out detailed kinetic studies, and therefore no attempt was made to assign the nature of the species.

The rate constant for the reaction of SeROH with ${}^{\bullet}$OH radical was determined by employing competition kinetics using isopropanol as reference solute (Table 1).[20] Since the ${}^{\bullet}$OH radical can also participate in H-abstraction from the alkyl groups or from the OH group of SeROH, it was necessary to assess the contribution of the radical formed by H-abstraction from SeROH.

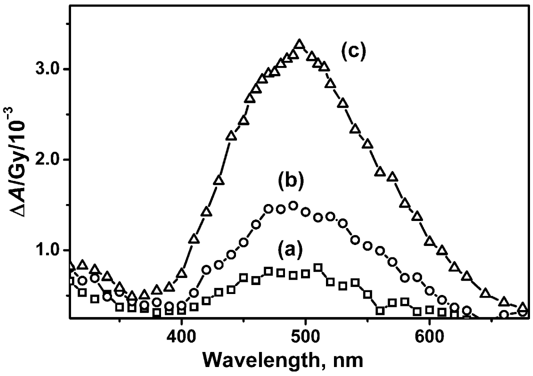

Figure 4. Transient spectra obtained at 5 μs after pulse radiolysis of N_2O-saturated aqueous solutions of: a) 50 μм, b) 100 μм, and c) 500 μм SeBOH at pH 7. Absorbed dose, (9.1 ± 0.2) Gy.

For this, the reaction of SeROH was performed with H atom at pH 1. The resultant transient spectrum did not show any absorbance at wavelength >300 nm, indicating that the species generated by H atom abstraction from the alkyl chain of SeROH did not absorb in the wavelength region where other selenium radicals absorb (Figure S6 in the Supporting Information).

The stability of the $(>\mathrm{Se}\therefore\mathrm{Se}<)^+$ radical can be understood from the equilibrium constant for the $(>\mathrm{Se}\therefore\mathrm{Se}<)^+$ radical formation, which was calculated according to the procedure described earlier.[9] As is evident from Table 1, the equilibrium constant for the $(>\mathrm{Se}\therefore\mathrm{Se}<)^+$ radical decreased in the order SeBOH > SeEOH > SePOH.

The trichloromethyl peroxyl radicals ($CCl_3O_2^{\bullet}$) radicals are model peroxyl radicals and can be conveniently generated by pulse radiolysis.[21] The transient absorption spectra generated on treatment of $CCl_3O_2^{\bullet}$ with SeROH showed an absorption maximum in the range from 480–500 nm similar to that observed with the ${}^{\bullet}$OH radical reaction (Figure S7 in the Supporting Information). The bimolecular rate constant for the reaction of $CCl_3O_2^{\bullet}$ with SeROH was estimated by employing competition kinetics using 2,2-azino-bis(3-ethylbenzthiazoline-6-sulfonate) ($ABTS^{2-}$) as reference solute (Table 1).[22]

2. Oxidizing versus reducing radicals

The radicals generated by different reactions of SeROH with ${}^{\bullet}$OH radicals can be both oxidizing and reducing in nature.[9,10]

Table 1. Estimated kinetic parameters for the reaction of ${}^{\bullet}$OH radical with SeROH compounds.

Compounds	Rate constant $(k)\times10^9$ $[\mathrm{M}^{-1}\,\mathrm{s}^{-1}]$		$(>\mathrm{Se}\therefore\mathrm{Se}<)^+$ decay rate $2k/\varepsilon l$ $[\mathrm{s}^{-1}]\times10^5$		Equilibrium constant $(K, [\mathrm{M}^{-1}])\times10^4$	
	$k_{\mathrm{SeROH}+{}^{\bullet}\mathrm{OH}}$	$k_{\mathrm{SeROH}+\mathrm{CCl3O2}\cdot}$	pH 1	pH 7	pH 1	pH 7
SeEOH	10.0 ± 0.1	0.48 ± 0.04	5.5 ± 0.2	9.4 ± 0.3	2.0 ± 0.2	1.1 ± 0.2
SePOH	7.3 ± 0.1	0.88 ± 0.03	4.2 ± 0.3	7.9 ± 0.2	0.8 ± 0.1	4.2 ± 0.3
SeBOH	9.7 ± 0.1	1.13 ± 0.06	3.7 ± 0.2	6.5 ± 0.2	3.5 ± 0.2	2.8 ± 0.3

The yield of the oxidizing radicals was estimated by their ability to oxidize ABTS^{2-} to produce ABTS$^{\bullet-}$ radical, absorbing at 645 nm. By following the rate of formation of ABTS$^{\bullet-}$ radical as a function of ABTS^{2-} concentration, the bimolecular rate constant for the reaction of $(>\mathrm{Se}\therefore\mathrm{Se}<)^{+}$ with ABTS^{2-} was estimated. For this, N_2O-saturated aqueous solutions at pH 7, containing 5 mM SeROH and 10–100 μM ABTS^{2-} were pulse irradiated (under these conditions the radicals are predominantly of $(>\mathrm{Se}\therefore\mathrm{Se}<)^{+}$ radical type) and by using the extinction coefficient of ABTS$^{\bullet-}$ ($\varepsilon_{645\mathrm{nm}} = 1.3\times10^{4}\,\mathrm{M}^{-1}\mathrm{cm}^{-1}$) and by applying Schuler's formula.[23] The radiation chemical yields (*G* value) of the $(>\mathrm{Se}\therefore\mathrm{Se}<)^{+}$ radicals were estimated and are given in Table 2. The rate constant for the oxidation of ABTS^{2-} by $(>\mathrm{Se}\therefore\mathrm{Se}<)^{+}$ radicals formed from SeBOH, SePOH and SeEOH at pH 7 were estimated and are listed in Table 2.

The $(>\mathrm{Se}^{\bullet+})$ and $(>\mathrm{Se}\therefore\mathrm{OH})$ radicals are known to undergo deprotonation/dehydration (path IIIb, Scheme 2) to form carbon-centered radicals of the type α-{bis(hydroxyl alkyl)}selenomethine radical that are reducing in nature (for convenience these radicals will be hence forth termed as α-reducing radicals).[9,10] The reducing ability of these radicals was followed by employing different redox systems. For this, initially an N_2O-saturated aqueous solution containing 4 mM of SeROH and varying concentration of (10–100 μM) methyl viologen (MV^{2+}) was pulse radiolyzed and the formation of MV$^{\bullet+}$ at 605 nm was monitored.[24]

The reaction system containing SeEOH did not show any signal at 605 nm, while that for SePOH and SeBOH formed MV$^{\bullet+}$ with a similar rate constant (within experimental limitations; Table 2). This confirmed that the α-reducing radicals from SeEOH are much less reducing than those from SePOH and SeBOH. A similar reaction pattern was observed with duroquinone (DQ) and thionine (Th^{2+}). The yield of the reducing radicals was estimated from the yield of these radicals using their reported extinction coefficient and are listed in Table 2 along with their bimolecular rate constants.[25,26]

3. Product analysis

The $(>\mathrm{Se}\therefore\mathrm{Se}<)^{+}$ radicals formed in the above reactions may undergo disproportionation to form selenoxide (SeROH$_{\mathrm{ox}}$; path V, Scheme 2) as one of the products.[27] Therefore, formation of SeROH$_{\mathrm{ox}}$ was analyzed in these reactions (Figure 5 and Figure S8 in the Supporting Information). The HPLC chromatogram indicated that SeEOH, SePOH and SeBOH were eluted at 4.4, 10.2 and 36.9 min, respectively, while the corresponding selenoxides were eluted at 2.8, 3.2 and 3.8 min, respectively. Using the calibration graphs, the yields of SeEOH$_{\mathrm{ox}}$, SePOH$_{\mathrm{ox}}$ and SeBOH$_{\mathrm{ox}}$ were estimated to be (0.20 ± 0.02), (0.26 ± 0.02) and (0.29 ± 0.03) μmol J^{-1}, respectively. Generally, selenoxides with the reactive β-methylene group are unstable and undergo *syn*-elimination, thus direct estimation of SeROH$_{\mathrm{ox}}$ may involve some errors.[6,13] Therefore, an indirect method using dithiothretol (DTT) conversion to oxidized DTT (DTT$_{\mathrm{ox}}$) by SeROH$_{\mathrm{ox}}$ was employed, where the yield of DTT$_{\mathrm{ox}}$ formed is equivalent to the SeROH$_{\mathrm{ox}}$ concentration.

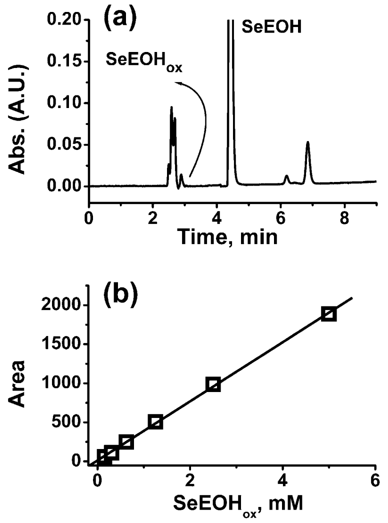

Figure 5. a) HPLC chromatogram showing the formation of SeEOH$_{\mathrm{ox}}$ after radiolytic degradation of an N_2O-saturated aqueous solution of 5 mM SeEOH. b) The calibration curve plotted by analysis of absorption peak area for the known concentrations of SeEOH$_{\mathrm{ox}}$.

DTT and DTT$_{\mathrm{ox}}$ were observed at 6.8 and 10.6 min (Figures S9–S11 in the Supporting Information), and the estimated radiation chemical yield of SeEOH$_{\mathrm{ox}}$, SePOH$_{\mathrm{ox}}$ and SeBOH$_{\mathrm{ox}}$ was (0.23 ± 0.02), (0.29 ± 0.02) and (0.31 ± 0.03) μmol J^{-1}, respectively. The yields of SeROH$_{\mathrm{ox}}$ estimated by both direct and indirect method are similar, indicating their stable nature. The results further signify that the yield of selenoxide increases with increasing alkyl chain length.

It has been reported that during the reaction of bis(2-ethanol)sulfide (SuEOH) with the $^{\bullet}$OH radical, formaldehyde (HCHO) is one of the major products with radiation chemical yield of approximately 0.27 μmol J^{-1}, which is 45 % of the initial $^{\bullet}$OH

Table 2. Rate constants and yield of oxidizing and reducing radicals formed during reaction of the $^{\bullet}$OH radical with SeROH compounds.

			SeEOH	SePOH	SeBOH
reaction with oxidizing radical (ABTS$^{\bullet-}$/ABTS^{2-}) ($E_0 = +0.67$ V)		yield [μmol J^{-1}]	0.22 ± 0.03	0.34 ± 0.02	0.31 ± 0.03
		rate constant (*k*) [M^{-1} s^{-1}]	$(6.0\pm0.3)\times10^{9}$	$(3.6\pm0.2)\times10^{9}$	$(4.1\pm0.2)\times10^{9}$
reaction with reducing radical	Th^{2+}/Th$^{\bullet+}$($E = +0.06$ V vs. NHE)	yield [μmol J^{-1}]	0.11 ± 0.02	0.13 ± 0.02	0.13 ± 0.01
		rate constant (*k*) [M^{-1} s^{-1}]	$(7.4\pm0.2)\times10^{8}$	$(2.6\pm0.3)\times10^{9}$	$(1.9\pm0.1)\times10^{9}$
	DQ/DQ$^{\bullet-}$ ($E = -0.26$ V vs. NHE)	yield [μmol J^{-1}]	no reaction	0.13 ± 0.01	0.15 ± 0.04
		rate constant (*k*) [M^{-1} s^{-1}]		(7.6 ± 0.3) x 10^{8}	$(2.0\pm0.2)\times10^{9}$
	MV^{2+}/MV$^{\bullet+}$ ($E = -0.44$ V vs. NHE)	yield [μmol J^{-1}]	no reaction	0.14 ± 0.02	0.17 ± 0.02
		rate constant (*k*) [M^{-1} s^{-1}]		$(9.4\pm0.5)\times10^{8}$	$(1.4\pm0.2)\times10^{9}$

radical yield. Anticipating a similar reaction, with the analogous selenium compound (path IV, Scheme 2), experiments were performed to detect HCHO and any other aldehydes in the form of hydrazone and were quantified by using HPLC, where dinitrophenylhydrazine (DNPH) and DNPH-HCHO were eluted at 5.1 and 7.4 min, respectively.[28] Using calibration plot for hydrazone, the yield of HCHO was estimated to be (0.11 ± 0.01) μmol J^{-1} for SeEOH, which corresponds to approximately 18 % of the initial $^{\bullet}$OH radical yield (Figure S12 in the Supporting Information). In case of SePOH and SeBOH the yield of HCHO was negligible ($<$0.005 μmol J^{-1}) and was less than 2 %, of the total $^{\bullet}$OH radical. This unusually lower yield of HCHO in SeEOH as compared to SuEOH suggests facile formation and higher stability of the $(>\mathrm{Se}\therefore\mathrm{Se}<)^{+}$ radical as compared to $(>\mathrm{S}\therefore\mathrm{S}<)^{+}$. In fact it was earlier reported by Bobrowski et al. that even at 0.1 M SuEOH, no $(>\mathrm{S}\therefore\mathrm{S}<)^{+}$ radical was observed at neutral pH.[29] The other products generated from the decay of α-{bis(hydroxyl alkyl)}selenomethine radical could not be quantified. The details of the reaction mechanism are depicted in Scheme 2.

4. Antioxidant activity

The stability and nature of a one-electron oxidized transient should reflect in their antioxidant activity, therefore the ability of SeROH to protect DNA from γ-radiation-induced damage was estimated. $^{\bullet}$OH-radical induced strand breaks in DNA leads to transformation of super-coiled double stranded DNA to linear and circular forms.[30] In the presence of compounds that have the ability to scavenge $^{\bullet}$OH radicals, the percentage conversion of the intact DNA to other forms should reduce. Therefore, in the present study, the effect of SeROH on $^{\bullet}$OH-radical induced DNA damage was assayed. Figure S13A–C in the Supporting Information shows the gel images of the electrophoretic pattern of the DNA samples treated with 8 Gy in the absence and presence of varying concentration (0.1–1 mM) of SeEOH, SePOH and SeBOH. From the images it is clear that all the three compounds showed protection towards radiation-induced DNA damage in a concentration-dependent manner. The percentage protection for a given concentration of selenium compounds was calculated by considering the damage caused by radiation as 100 % and calculating the ratio of intact DNA with respect to DNA control. The IC_{50} value, that is, the concentration required to protect DNA from radiation-induced damage by 50 % was estimated to be 0.60 and 0.58 mM for SePOH and SeBOH, respectively, while for SeEOH, the IC_{50} value was $>$1 mM (Figure S13D in the Supporting Information).

At a fixed concentration of 1 mM, the respective DNA protection exhibited by SeEOH, SePOH and SeBOH are listed in Table 3.

The antioxidant activity of SeROH compounds was also evaluated in terms of their GPx-like activity, by monitoring their reaction with hydrogen peroxide, using glutathione (GSH)–glutathione disulfide (GSSG)–nicotinamide adenine dinucleotide phosphate (NADPH) coupled assay, measuring the initial velocity (v) for the decay of NADPH at 345 nm (Figure S14 in the Supporting Information).[31] At a fixed concentration of SeROH (0.1 mM), the decay rate at 345 nm increased with an increase in alkyl chain length and followed the pattern SeBOH $>$ SePOH $>$ SeEOH (Table 3).

Table 3. Antioxidant parameters of SeROH compounds.

	SeEOH	SePOH	SeBOH
GPx activity initial velocity (v) [μmol s^{-1}]	3.8 ± 0.2	5.5 ± 0.2	6.3 ± 0.3
DNA protection [%][a] (SeROH = 1 mM)	43 ± 3	64 ± 5	72 ± 5

[a] $P < 0.01$ versus radiation control, calculated with the Student's t-test.

5. Quantum chemical calculations

To compliment the experimental results obtained from pulse radiolysis, energetics for the possible reaction pathways during the $^{\bullet}$OH radical reaction with SeROH was calculated by employing quantum chemical calculations at the B3LYP/6-31 + G(d,p) level (Becke nonlocal model and Lee–Yang–Parr exchange-correlation functionals).[32,33] Optimized ground-state geometry of SeROH belongs to the C1 point group and did not show any interaction between Se and the oxygen atom of the hydroxyl group. In all SeROH compounds, the highest occupied molecular orbital (HOMO) was found to be localized on the selenium atom; therefore an electrophile like the $^{\bullet}$OH radical would react mainly on the Se atom. The HOMO values of SeROH compounds are summarized in Table S1 in the Supporting Information. Similarly, the geometry of all the possible transients formed during the $^{\bullet}$OH radical reaction with SeROH was optimized at the same calculation level. From the estimated energy of the optimized structures of SeROH and their respective transients, the change in energy for all the possible reactions was calculated (Table 4 and Schemes S1–S3 in the Supporting Information). The initial step for the formation of the $(>\mathrm{Se}\therefore\mathrm{OH})$ radical (path I, Scheme 2) on reaction of the $^{\bullet}$OH radical with SeROH was endothermic. Conversion of the $(>\mathrm{Se}\therefore\mathrm{OH})$ radical to $(>\mathrm{Se}^{\bullet+})$ can be either by self-dissociation (path IIa, Scheme 2) or by acid-catalyzed dehydration (path IIb, Scheme 2). The calculations, as given in Table 4, indicate that the acid catalysis is energetically more favorable than the spontaneous dissociation of $(>\mathrm{Se}\therefore\mathrm{OH})$. The results also show that $>\mathrm{Se}^{\bullet+}$ derived from SePOH and SeBOH can acquire stabilization through formation of five and six-membered rings, respectively, by the interaction of the lone pair of the oxygen with the selenium center (path IIIc, Scheme 2). Further, $>\mathrm{Se}^{\bullet+}$, can decay by two competing reactions: 1) formation of the 2c–3e bonded $(>\mathrm{Se}\therefore\mathrm{Se}<)^{+}$ radical (path IIIa, Scheme 2), and 2) irreversible loss of proton to form α-reducing radicals (path IIIb, Scheme 2). As seen from Table 4, conversion of $(>\mathrm{Se}^{\bullet+})$ to the $(>\mathrm{Se}\therefore\mathrm{Se}<)^{+}$ radical is exothermic while that to α-reducing radical is endothermic, indicating that the former reaction is more favorable compared to the latter. On close examination of the optimized structure of $(>\mathrm{Se}^{\bullet+})$ derived from SeEOH, it can be observed that the distance between the selenium center and the hydrogen atom present at the α-carbon atom

Table 4. Calculated energy changes for different reactions involving $^{\bullet}OH$ radicals with SeROH.

Transients reactions	B3LYP energy change (ΔE, kcal mol^{-1})					
	SeEOH	SePOH	SeBOH	SuEOH	SuPOH	SuBOH
$>Se + {}^{\bullet}OH \rightarrow (>Se \therefore OH)$	3.49	4.51	7.94	173.81	134.58	258.89
$(>Se \therefore OH) \xrightarrow{H_3O^+} >Se^{\bullet+} + 2\,H_2O$	−82.53	−90.56	−89.60	−82.45	−96.72	−98.71
$(>Se \therefore OH) \rightarrow >Se^{\bullet+} + OH^-$	356.02	340.78	349.56	350.53	347.11	340.79
$>Se^{\bullet+} \xrightarrow{H_2O} \alpha$-reducing radical $+ H_3O^+$	115.03	107.84	115.63	109.45	120.31	115.98
$>Se^{\bullet+} \xrightarrow{>Se} (>Se \therefore Se<)^+$	−14.89 (6.81)[a]	−11.57 (2.29)[a]	−16.68 (−3.78)[a]	151.68 (150.77)[a]	122.21 (120.98)[a]	236.37 (235.22)[a]
$2\,(>Se \therefore Se<)^+ \xrightarrow{3\,H_2O} >Se{=}O +$ $3 >Se + 2\,H_3O^+$	18.45 (−24.95)[a]	20.87 (−6.85)[a]	23.62 (−2.18)[a]	34.57 (32.75)[a]	39.37 (36.91)[a]	36.70 (34.44)[a]

[a] The values in the parenthesis are BSSE (for dimer radical cation) corrected.

is less than that of the sum of their van der Waals radii, indicating the presence of nonbonding interactions.

The energy of such nonbonded interaction (E_{nb}) can be extrapolated by performing the NBO analysis of the orbitals on the ($>Se^{\bullet+}$) radical.[34] E_{nb} represents the perturbation induced by the delocalization of the electron density in a bond and the value can be directly correlated to the strength of interaction. The NBO analysis indicated that the σ-orbital of α-C–H interacts with the σ* orbital centered at the Se atom with E_{nb} of 1.61 kcal mol^{-1}. In case of SePOH and SeBOH, the σ-orbital of α-C–H interacts with the σ* orbital of Se–O bond with E_{nb} of 1.41 and 1.32 kcal mol^{-1}, respectively.

Discussion

Initial research in the design of selenium antioxidants was concentrated mainly on GPx-like activity, where the reaction with molecular oxidants like hydroperoxides was crucial.[13,14] However, recent research recognizes the necessity to know the role of one-electron transfer processes in the antioxidant activity, where involvement of free radical oxidants is important. With this aim, our group has been investigating the reactions of free radicals, like $^{\bullet}OH$, with several functionalized selenium compounds using pulse radiolysis technique. In the present investigation we have focused on bis(alkanol)selenides (SeROH) of three different alkyl chain lengths, SeEOH, SePOH and SeBOH.

The results indicate that the initial reaction of $^{\bullet}OH$ radical takes place at the selenium center, producing three different types of radicals like hydroxyselenouranyl radical ($>Se \therefore OH$), selenium centered radical cation ($>Se^{\bullet+}$), dimer radical cation $(>Se \therefore Se<)^+$ and α-{bis(hydroxyl alkyl)}selenomethine radical (α-reducing radical). The relative reactivity and yield of the transients depend upon the alkyl chain length.

The $(>Se \therefore Se<)^+$ radical from all the three SeROH exhibits broad transient absorption with maxima in the range of 460 to 500 nm. The K_{eq} value for $(>Se \therefore Se<)^+$ radical formation, which also indicates their relative stability, was higher for SeBOH as compared to SeEOH or SePOH. The lower value of K_{eq} for SePOH is also due to the formation of ($>Se^{\bullet+}$) radical, which can acquire stabilization through the formation of a kinetically stable five-membered ring. Such radicals in case of SeEOH would form an unstable four-membered ring, while that for SeBOH result in a six-membered ring. The latter, although stable thermodynamically, is generally not observed in transient absorption studies. The $(>Se \therefore Se<)^+$ radical decayed by radical–radical reaction, where the rate constant was higher for SeEOH compared to SePOH and SeBOH. Subsequent to the radical-radical reactions, they undergo hydrolysis to form SeROH$_{ox}$ as the major product.[27] The estimated yields under the radiolysis conditions were 40.3, 49.0 and 51.6% of the total yield of the $^{\bullet}OH$ radical, respectively, for SeEOH$_{ox}$, SePOH$_{ox}$ and SeBOH$_{ox}$. If SeROH$_{ox}$ is formed only by the radical–radical decay of $(>Se \therefore Se<)^+$, its yield should always be less than 50% of the yield of $^{\bullet}OH$. Marginally higher yields for SePOH and SeBOH indicate that other pathways such as hydrolysis of radical cations and reaction with radiolytically generated hydrogen peroxide may contribute to its formation.

A strikingly interesting observation for selenium as compared to similar sulfur compounds is that selenium compounds are nearly quantitatively converted to selenoxides while no sulfoxides could be reported with sulfur analogues.[29] This property plays an important role in imparting catalytic antioxidant activity in selenium compounds.

The ($>Se^{\bullet+}$), which is in equilibrium with the $(>Se \therefore Se<)^+$ radical, can undergo proton loss to form α-reducing radical. The reducing ability of such radicals derived from SeBOH is also higher as compared to those derived from SePOH and SeEOH. This may be the consequence of the presence of the electron-donating alkyl hydroxyl moiety attached to the α-carbon atom. The ($>Se \therefore OH$) radical derived from SeEOH, like the analogous sulfur radical, can undergo a Barton-type reaction to form HCHO. However, the estimated yield of HCHO was found to be four times lower than that for SuEOH.[18] This indicates that the ($>Se \therefore OH$) radical of SeEOH preferentially forms $(>Se \therefore Se<)^+$, due to higher stabilization of this species as seen from quantum chemical calculations. In case of SePOH and SeBOH, no detectable amount of HCHO was observed as their corresponding ($Se \therefore OH$) adducts form less stable seven- and eight-membered ring species, respectively. Formation of carbon-centered radicals and aldehydes can lead to increased oxidative stress through the formation of peroxyl radicals and Schiff reactions with amino acids, respectively.[2,10,35] The negligible contribution from these species in case of selenium compounds as compared to their sulfur analogues further ascertains that selenium is a better antioxidant than sulfur.

The rate constants for the reaction of SeROH with peroxyl radicals and their relative GPx activity showed linear correlation with their HOMO energy levels (TableS1 in the Supporting Information). This along with the results reported for many other selenium compounds, prompted us to believe that, the antioxidant activity is initiated mainly by a single-electron-transfer reaction, a process which is not considered very important by many as compared to the two-electron transfer or oxygen-transfer reactions.

These compounds were also tested for in vitro antioxidant activity by means of protecting plasmid pBR322 DNA from γ-radiation induced damage. All compounds showed protection at high (millimolar) concentrations. This may be due to direct scavenging of $^{\bullet}$OH radical, which may not be of great significance. However, in the cellular systems, with the presence of high amounts of thiols, one would expect reversible reduction of selenoxides by the thiols, providing catalytic antioxidant mechanism. The observations from antioxidant studies confirm that, SeBOH which gives higher yield of SeBOH$_{ox}$, exhibits better ability to scavenge ROS. In order to understand this significantly different activity of selenium over sulfur, we made detailed analysis of the nature of radicals and their structures by quantum chemical calculations at B3LYP/6-31+G(d,p) level. It is well established that the sulfur/selenium centered radical cations are stabilized by forming 2c–3e bonds. In this, the orbital with the lone-pair electron (either the suitable heteroatom like N or O or another sulfur/selenium atom) mix with another orbital containing an unpaired electron on sulfur/selenium to form a hemibond.[36] In such hemibond formation, there are two electrons in the bonding orbital and one electron in the antibonding orbital, which tends to cause mutual repulsion between the two bonding atoms. In selenium, the orbitals are more diffused as compared to sulfur, thereby reducing the orbital overlap and repulsion and thus imparting higher stability to selenium-centered radicals. Also, the higher covalent radius in selenium reduces steric congestion at the selenium center as compared to sulfur. These unique features allow the selenium atom to readily form the $(>Se\therefore Se<)^+$ radical to an extent that other intermediates like $(>Se\therefore OH)$ and $(>Se^{\bullet+})$ are not observed. For the same reasons, sulfur analogues do not show $(>S\therefore S<)^+$ radical formation even at a concentration of 0.1 M.[29] The quantum chemical calculations support these observations, where the calculated enthalpy change for formation of $(>Se\therefore Se<)^+$-type radical is exothermic, while it is endothermic for $(S\therefore S<)^+$ radicals.

In sulfur compounds the $(>S^{\bullet+})$-type radical undergoes deprotonation, which is facilitated in molecules where the *p*-orbital of the oxidized sulfur overlaps efficiently with the σ-orbital of the C–H bond.[36] As the orbitals present on selenium are more diffused than sulfur, a poor overlap with the σ-C–H orbital takes place leading to lower deprotonation. This was clearly observed in the NBO analysis, where the interaction between the chalcogen atoms with the neighboring C–H bond is higher in case of sulfur as compared to selenium compounds. On close examination of the optimized structure of $(>S^{\bullet+})$ of SuEOH, it can be observed that the distance between the sulfur center and the hydrogen atom present at the α-carbon atom is less than that for $(>Se^{\bullet+})$ of SeEOH. The E_{nb} value is 1.5-times higher as compared to SeEOH. Higher E_{nb} values in sulfur compounds with the −α methylene group leads to elongation and easy cleavage of the C–H bond resulting in higher radiolytic degradation as compared to analogous selenium compounds. The higher α-reducing radical seen in sulfur compounds is also due to its lower affinity to form $(>S\therefore S<)^+$ radical. All these calculations support the experimentally observed pulse radiolysis results and the products formed.

Conclusions

The bis(alkanol)selenides react with the $^{\bullet}$OH radical to form $(>Se\therefore Se<)^+$ radicals primarily, which depending on the alkyl chain length undergo transformation to produce selenoxides (SeROH$_{ox}$) as an important reaction products. Earlier it was presumed that the formation of selenoxide occurs only by oxygen atom transfer, our results confirm that the selenide–selenoxide conversion can be initiated by a one-electron oxidation process. The experimental results combined with the calculations proved that selenium compound with higher HOMO energy level, formed more stable $(>Se\therefore Se<)^+$ radicals and produced higher yields of SeROH$_{ox}$. Such compounds also exhibit better antioxidant activity, a property which is clearly not observed in analogous sulfur compounds. The SeROH$_{ox}$ formed during these reactions can be reduced back to SeROH in the presence of reducing agents like thiols, thereby imparting catalytic activity. The results therefore provide a unique example of how probing single-electron-transfer processes in real time scales, can be utilized to design selenium-based antioxidants, where the free radical as well GPx-like activity can be correlated with synergistic effect.

Experimental Section

Materials

GSH, GSSG, glutathione reductase (GR), NADPH, ABTS^{2-}, DTT, DTT$_{ox}$, MV^{2+}, sodium azide and DQ (>99%) were purchased from Sigma–Aldrich. DNPH was purchased from Sisco Research Laboratories and recrystallized from ethanol prior to use. HPLC grade acetonitrile, trifluoroacetic acid (TFA) and HCHO were purchased from Advent, India. All the other chemicals and reagents were of "Analar" grade and were used as such. The solutions were freshly prepared for each experiment in nanopure water with a conductivity of 0.1 μS cm^{-1}, obtained from a milipore water purification system. The pH of the solutions was adjusted using monosodium phosphate (NaH$_2$PO$_4$), disodium phosphate (Na$_2$HPO$_4$·2H$_2$O) and perchloric acid (HClO$_4$).

The SeROH were synthesized by the reported method (see the Supporting Information).[37] The corresponding selenoxide was synthesized by treating SeROH with 1.5 equivalents of hydrogen peroxide (H$_2$O$_2$) and characterized by NMR spectroscopy (^{1}H, ^{13}C and ^{77}Se; Figures S14–S16). The characterization details of SeROH are given in the Supporting Information. NMR spectra were recorded on a Bruker Avance-II 300 MHz spectrometer operating at 300.13 (^{1}H) and 57.25 MHz (^{77}Se{^{1}H}). ^{1}H NMR chemical shifts were relative to internal DMSO peak ($\delta = 2.49$ ppm). The ^{77}Se{^{1}H} NMR chemical shifts were relative to external diphenyl diselenide (Ph$_2$Se$_2$) in CDCl$_3$ ($\delta = 463.0$ ppm relative to Me$_2$Se (0 ppm)). UV–visible absorption studies were measured on a JASCO V-630 spectrophotometer. High performance liquid chromatographic (HPLC) measurements were carried out on a ELICO HL 460 HPLC system. Depending upon the experimental requirement, two different ^{60}Co γ-radiation sources were employed, that is, for the DNA nicking assay, a low dose rate source operating at 1 Gy min^{-1} was used, while for other experiments, ^{60}Co γ-source with a dose rate of 40 Gy min^{-1} was used.

Pulse radiolysis studies

Pulse radiolysis studies were carried out by using a 7 MeV electron beam with 100 ns pulse width.[26] Thiocyanate dosimeter (aerated aqueous solution of 10 mm KSCN, $G\varepsilon$ 475 nm $= 2.59\times10^{-4}$ m^2 J^{-1}) was used to estimate the absorbed dose and an average dose of 9 Gy per pulse was used for all experiments, unless otherwise stated.[38] The reaction with $^{\bullet}$OH radical was carried out in N_2O saturated solution, where $e^{\simeq}_{\mathrm{aq}}$ is quantitatively converted to $^{\bullet}$OH radical to give the final G_{OH} of 0.6 μmole J^{-1}.[39] The one-electron oxidation reactions were studied by using $N_3^{\bullet}$ radical, a specific one-electron oxidant generated by treatment of $^{\bullet}$OH with 0.1 m sodium azide (NaN_3). $CCl_3O_2^{\bullet}$ radicals were generated by radiolysis of aerated aqueous solution containing 48 % isopropanol and 4 % carbon tetrachloride at neutral pH. Under the experimental condition, the radiochemical yields (G) of $N_3^{\bullet}$ and $CCl_3O_2^{\bullet}$ radicals were 0.69 and 0.64 μmol J^{-1}, respectively.[40,41] The bimolecular rate for the reaction of SeROH with $CCl_3O_2^{\bullet}$ radical was estimated by employing competition kinetics using ABTS^{2-} as standard ($\varepsilon_{645\mathrm{nm}} = 1.35\times10^4$ m^{-1} cm^{-1}).

High performance liquid chromatographic (HPLC) analysis

The products obtained on $^{\bullet}$OH radical induced oxidative degradation of SeROH were identified and their yield was estimated by using HPLC. For this, N_2O saturated aqueous solutions of 5 mm SeROH were irradiated using ^{60}Co γ-source with a dose of 0.83 kGy. To avoid further reaction of the products, the irradiation dose was set in such a way that not more than 10 % of reactants underwent radiolysis. HCHO and selenoxide were the anticipated products obtained during radiolysis and were separated by isocratic method on a Prontosil 120-5-C18 reverse phase column and detected with an absorption detector.

The yield of HCHO was estimated by treating it with DNPH to form DNP-HCHO hydrazone which was detected by measuring its absorbance at 345 nm.[28] The radiated solutions (150 μL) were mixed with 50 μL DNPH (4 mm dissolved in 10 mm HCl) and stirred for 5 min. An aliquot (20 μL) of this reaction mixture was injected in the HPLC and eluted with acetonitrile/water (60:40; v/v) mixture containing 0.1 % TFA as mobile phase. The standard calibration curve was obtained from known concentration of HCHO derivatized with DNPH.

Selenoxide was estimated by two methods. In the direct method, the yield of the selenoxide formed during radiolysis was separated by HPLC using an acetonitrile/water mixture in the ratio 5:95 (v/v) with 0.1 % TFA as eluent, monitored at 240 nm. The yield was calculated from the calibration curve obtained from injecting known concentration of pure selenoxides. In the second method, the selenoxide formed was estimated by reaction with DTT, monitoring the formation of $\mathrm{DTT_{ox}}$, eluted and monitored by using similar experimental conditions used in the direct method. The yield of $\mathrm{DTT_{ox}}$ is equivalent to the amount of selenoxide formed and was estimated from the standard calibration curve obtained for $\mathrm{DTT_{ox}}$.

DNA nicking assay

$^{\bullet}$OH-radical induced DNA damage was studied by separating super coiled pBR322 DNA from the linear form by using gel electrophoresis.[30] For this, 1 μL of pBR322 (250 ng μL^{-1}) was mixed with different concentrations of SeROH and the final volume was made up to 20 μL. This solution was exposed to γ-radiation with a total dose of 8 Gy using a ^{60}Co γ-source. Reaction samples were mixed with 4 μL of bromophenol loading dye (6×). An equal volume (20 μL) of each sample was loaded on a 1.5 % agarose gel stained with ethidium bromide and subjected to electrophoresis. Gel images were taken using a UV transilluminator and analyzed with the GeneTools software (Version 08-3d.3.SynGene). The data given are mean ± S.E.M. from two independent experiments; each one assayed in triplicate. The statistical significance of the results was checked with the Student t-test.

GPx activity

GPx activity of SeROH compounds was calculated by using the NADPH-GSH-GSSG coupled assay.[30] Briefly, 2 mm H_2O_2 was added to 1 mm GSH solution containing 0.3 mm NADPH, 5 units mL^{-1} GR and 0.1 mm of SeROH dissolved in pH 7.4 phosphate buffers. The reaction was monitored by following a decrease in absorbance of NADPH at 340 nm as a function of time.

Quantum chemical calculations

The geometry of the proposed transients were optimized in gaseous phase by extensive variation in initial confirmation of the transients at B3LYP/6–31 + G(d,p) (Becke non-local model and Lee–Yang–Parr exchange correlation functionals) level. B3LYP is a hybrid functional and gives vibrational force fields, frequencies, and spectra, as well as thermochemical properties, with better accuracy.[42] 6–31 + G(d,p) is a well explored basis set attached with double diffusion functions for better results on reaction chemistry calculations of organic molecules involving free or lone pairs of electrons. The most stable transient structures were further optimized in water using polarizable continuum (PCM) solvent density (SMD) model.[43] SMD model includes calculation of cavitation and dispersion–repulsion energies and particularly useful when calculating free energy of solvation for a molecule going from a gas phase to solvent phase. The optimized structures were verified as global minima structures by performing the frequency calculation (see the Supporting Information). The energetics of the reactions was calculated by estimating the difference in the zero-point corrected B3LYP energy of the products and the reactants. All these calculations were performed by adopting the GAMESS suite of programs on a PC-based LINUX cluster platform.[44] Visualization of the geometry and relevant molecular orbitals was carried out by following the Chemmissian software (version V4.38). The B3LYP energy obtained for dimer radical cations of selenium and sulfur compounds was corrected for BSSE (basis-set superposition error) using counter-poise method. The BSSE correction values were 0.91, 1.23 and 1.15 kcal mol^{-1} for SuEOH, SuPOH and SuBOH dimer radical cations, respectively. Similarly BSSE correction values for SeEOH, SePOH and SeBOH were 21.7, 13.86 and 12.9 kcal mol^{-1}, respectively. To estimate the strength of non-bonding interactions (E_{nb}), natural bond order (NBO) analysis was carried out at the B3LYP/6–31 + G (d,p) level by using a Gaussian 09.[45]

Acknowledgements

The authors thank the Computer Center, BARC, for providing ANUPAM parallel computing facility. P.K. acknowledges CSIR for the senior research fellowship. The authors acknowledge Dr. D. K. Maity, HBNI, for initial training in computations and Dr. Ayesha Khan, Chemistry Department, Savitribai Phule Pune University, India for her help in Gaussian calculations.

Keywords: antioxidants · pulse radiolysis · radical reactions · selenides · selenoxides

[1] C. Winterbourne, *Nat. Chem. Biol.* **2008**, *4*, 278 – 286.
[2] E. E. Battin, J. L. Brumaghim, *Cell Biochem. Biophys.* **2009**, *55*, 1 – 23.
[3] G. Hardy, I. Hardy, *Nutrition* **2004**, *20*, 590 – 593.
[4] L. Flohe, W. A. Gunzler, H. H. Schock, *FEBS Lett.* **1973**, *32*, 132 – 134.
[5] V. N. Gladyshev, K. T. Jeang, T. C. Stadtman, *Proc. Natl. Acad. Sci. USA* **1996**, *93*, 6146 – 6151.
[6] L. A. Wessjohann, A. Schneider, M. Abbas, W. Brandt, *Biol. Chem.* **2007**, *388*, 997 – 1006.
[7] A. J. Mukherjee, S. S. Zade, H. B. Singh, R. B. Sunoj, *Chem. Rev.* **2010**, *110*, 4357 – 4416.
[8] B. G. Singh, E. Thomas, S. N. Sawant, K. Takahashi, K. Dedachi, M. Iwaoka, K. I. Priyadarsini, *J. Phys. Chem. A* **2013**, *117*, 9259 – 9265.
[9] B. G. Singh, S. A. Nadkarni, V. K. Jain, K. I. Priyadarsini, *RSC Adv.* **2015**, *5*, 66621 – 66627.
[10] B. Mishra, A. Sharma, S. Naumov, K. I. Priyadarsini, *J. Phys. Chem. B* **2009**, *113*, 7709 – 7715.
[11] B. Mishra, L. B. Kumbhare, V. K. Jain, K. I. Priyadarsini, *J. Phys. Chem. B* **2008**, *112*, 4441 – 4446.
[12] B. Mishra, D. K. Maity, K. I. Priyadarsini, H. Mohan, J. P. Mittal, *J. Phys. Chem. A* **2004**, *108*, 1552 – 559.
[13] F. Kumakura, B. Mishra, K. I. Priyadarsini, M. Iwaoka, *Eur. J. Org. Chem.* **2010**, 440 – 445.
[14] L. Orian, S. Toppo, *Free Radical Biol. Med.* **2014**, *66*, 65 – 74.
[15] B. Mishra, K. I. Priyadarsini, H. Mohan, G. Mugesh, *Bioorg. Med. Chem. Lett.* **2006**, *16*, 5334 – 5338.
[16] B. G. Singh, E. Thomas, F. Kumakura, K. Dedachi, M. Iwaoka, K. I. Priyadarsini, *J. Phys. Chem. A* **2010**, *114*, 8271 – 8277.
[17] M. Bonifacic, I. Stefanic, G. L. Hug, D. A. Armstrong, K. D. Asmus, *J. Am. Chem. Soc.* **1998**, *120*, 9930 – 9940.
[18] C. Schoneich, K. Bobrowski, *J. Am. Chem. Soc.* **1993**, *115*, 6538 – 6547.
[19] Z. B. Alfassi, R. H. Schuler, *J. Phys. Chem.* **1985**, *89*, 3359 – 3363.
[20] W. Wang, M. N. Schuchmann, H. P. Schuchmann, W. Knolle, J. von Sonntag, C. von Sonntag, *J. Am. Chem. Soc.* **1999**, *121*, 238 – 245.
[21] T. N. Das, K. I. Priyadarsini, *J. Phys. Chem.* **1994**, *98*, 5212 – 5278.
[22] B. S. Wolfenden, R. L. Willson, *J. Chem. Soc. Perkin Trans. 1* **1982**, *11*, 805 – 812.
[23] R. H. Schuler, A. L. Hartzell, B. Behar, *J. Phys. Chem.* **1981**, *85*, 192 – 199.
[24] S. Solar, W. Solar, N. Getoff, J. Holcman, K. Sehested, *J. Chem. Soc. Faraday Trans.* **1982**, *78*, 2467 – 2477.
[25] D. Meisel, G. Czapski, *J. Phys. Chem.* **1975**, *79*, 1503 – 1509.
[26] S. N. Guha, P. N. Moorthy, K. Kishore, D. B. Naik, K. N. Rao, *Proc. Indian Acad. Sci. Chem. Sci.* **1987**, *99*, 261 – 271.
[27] C. Schoneich, A. Aced, K. D. Asmus, *J. Am. Chem. Soc.* **1993**, *115*, 11376 – 11383.
[28] A. Soman, Y. Qiu, Q. Chan Li, *J. Chromatogr. Sci.* **2008**, *46*, 461 – 465.
[29] K. Bobrowski, G. L. Hug, B. Marciniak, B. Miller, C. Schoneich, *J. Am. Chem. Soc.* **1997**, *119*, 8000 – 8011.
[30] R. Ragagopalan, K. Wani, N. G. Huigol, T. V. Kagiya, C. K. Krishnannair, *J. Radiat. Res.* **2002**, *43*, 153 – 159.
[31] M. Maiorinoa, A. Roveria, F. Ursini, C. Gregolin, *J. Free Radicals Biol. Med.* **1985**, *1*, 203 – 207.
[32] O. Makogon, R. Flyunt, T. Tobien, S. Naumov, M. Bonifacic, *J. Phys. Chem. A* **2008**, *112*, 5908 – 5916.
[33] B. K. Sarma, G. Mugesh, *ChemPhysChem* **2009**, *10*, 3013 – 3020.
[34] M. Iwaoka, H. Komatsu, T. Katsuda, S. Tomoda, *J. Am. Chem. Soc.* **2004**, *126*, 5309 – 5317.
[35] P. A. Grimsrud, H. Xie, T. J. Griffin, D. A. Bernlohr, *J. Biol. Chem.* **2008**, *283*, 21837 – 21841.
[36] K. D. Asmus, in *Radiation Chemistry: Present Status and Future Trends*, (Eds.: C. D. Jonah, B. S. M. Rao), Elsevier, Amsterdam, **2001**, pp. 341 – 394.
[37] S. Dey, N. Ghavale, A. S. Hodage, V. K. Jain, G. Kedarnath, L. B. Kumbhare, P. P. Phadnis, P. C. Parashiva, K. I. Priyadarsini, A. Wadawale, Bhabha Atomic Research Centre, document BARC/**2009**/I/003.
[38] G. V. Buxton, C. C. Stuart, *J. Chem. Soc. Faraday Trans.* **1995**, *91*, 279 – 281.
[39] G. V. Buxton, Q. G. Mulazzani, in *Radiation: Chemical Techniques*, Wiley-VCH, Weinheim, Germany, **2001**, pp. 503 – 557.
[40] R. Zhao, J. Lind, G. Merenyi, T. E. Eriksen, *J. Am. Chem. Soc.* **1998**, *120*, 2811 – 2816.
[41] X. Shen, J. Lind, T. E. Eriksen, *J. Phys. Chem.* **1989**, *93*, 553 – 557.
[42] P. J. Stephens, F. J. Devlin, *J. Phys. Chem.* **1994**, *98*, 11623 – 11627.
[43] A. V. Marenich, C. J. Cramer, D. G. Truhlar, *J. Phys. Chem. B* **2009**, *113*, 6378 – 6396.
[44] M. W. Schmidt, K. K. Baldridge, J. A. Boatz, S. T. Elbert, M. S. Gordon, J. H. Jensen, S. Koseki, N. Matsunaga, K. A. Nguyen, S. J. Su, T. L. Windus, M. Dupuis, J. A. Montgomery, *J. Comput. Chem.* **1993**, *14*, 1347 – 1358.
[45] M. J. Frisch, G. W. Trucks, H. B. Schlegel, G. E. Scuseria, M. A. Robb, J. R. Cheeseman, G. Scalmani, V. Barone, B. Mennucci, G. A. Petersson, H. Nakatsuji, M. Caricato, X. Li, H. P. Hratchian, A. F. Izmaylov, J. Bloino, G. Zheng, J. L. Sonnenberg, M. Hada, M. Ehara, K. Toyota, R. Fukuda, J. Hasegawa, M. Ishida, T. Nakajima, Y. Honda, O. Kitao, H. Nakai, T. Vreven, J. A. Montgomery, Jr., J. E. Peralta, F. Ogliaro, M. Bearpark, J. J. Heyd, E. Brothers, K. N. Kudin, V. N. Staroverov, R. Kobayashi, J. Normand, K. Raghavachari, A. Rendell, J. C. Burant, S. S. Iyengar, J. Tomasi, M. Cossi, N. Rega, J. M. Millam, M. Klene, J. E. Knox, J. B. Cross, V. Bakken, C. Adamo, J. Jaramillo, R. Gomperts, R. E. Stratmann, O. Yazyev, A. J. Austin, R. Cammi, C. Pomelli, J. W. Ochterski, R. L. Martin, K. Morokuma, V. G. Zakrzewski, G. A. Voth, P. Salvador, J. J. Dannenberg, S. Dapprich, A. D. Daniels, Ö. Farkas, J. B. Foresman, J. V. Ortiz, J. Cioslowski, D. J. Fox, Gaussian, Inc., Wallingford CT, 2009.

Received: April 25, 2016

FULL PAPER

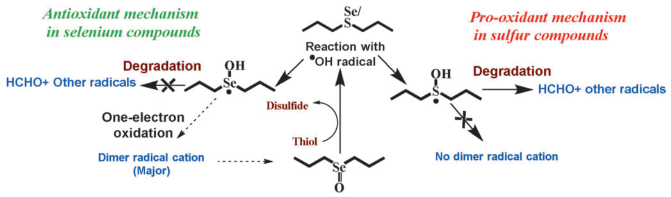

Roots radicals: Functionalized alkyl selenides react with hydroxyl radical to form dimer radical cation, which is converted to a selenoxide that is catalytically recycled by thiols. Comparing these results with those for sulfur analogues confirmed for the first time the distinctive role of selenium in making such compounds better antioxidants.

Redox Chemistry

P. V. Kumar, B. G. Singh, P. P. Phadnis,*
*V. K. Jain, K. I. Priyadarsini**

■■ – ■■

Effect of Molecular Interactions on Electron-Transfer and Antioxidant Activity of Bis(alkanol)selenides: A Radiation Chemical Study